Published in J. Vac. Sci. Technol. B 19, 1644 (2001).

Distribution of Nitrogen Atoms in Dilute GaAsN and InGaAsN Alloys studied by Scanning Tunneling Microscopy

H. A. McKay and R. M. Feenstra
Department of Physics, Carnegie Mellon University, Pittsburgh, Pennsylvania 15213
T. Schmidtling and U. W. Pohl
Technische Universität Berlin, Hardenbergstr. 36, D-10623 Berlin, Germany
J. F. Geisz
National Renewable Energy Laboratory, Golden, Colorado 80401

Abstract

Nitrogen atoms in the cleaved $(1\bar{1}0)$ surfaces of dilute GaAsN and InGaAsN alloys have been studied using cross-sectional scanning tunneling microscopy. The distribution of nitrogen atoms in $GaAs_{0.983}N_{0.017}$ and $In_{0.04}Ga_{0.96}As_{0.99}N_{0.01}$ alloys is found to be in agreement with random statistics, with the exception of a small enhancement in the number of [001]-oriented nearest neighbor pairs. The effects of annealing on $In_{0.04}Ga_{0.96}As_{0.99}N_{0.01}$ alloys has been studied by scanning tunneling spectroscopy. Spectra display a reduced band gap compared to GaAs but little difference is seen between as-grown versus annealed InGaAsN samples. In addition, voltage dependent imaging has been used to investigate second-plane nitrogen atoms.

1 Introduction

GaAsN and InGaAsN alloys with low N content demonstrate large band gap bowing with only a few % N content. Typical optical bowing coefficients for semiconductor alloys are on the order of 0.1 eV and are fairly insensitive to composition. In contrast, bowing coefficients for GaAsN and InGaAsN alloys can be on the order of 10 eV and vary strongly with composition [1]. Considerable band gap reduction with modest N content is possible. Applications for these materials include lasers with wavelength in the 1.3-1.5 μm range as well as solar cells with band gaps around 1.0 eV [2]. Though the materials are promising for optoelectronic devices they have displayed evidence of inhomogeneities, such as broad photoluminescence (PL) line widths, variable PL decay times and short minority carrier diffusion lengths [3-6]. These characteristics have been interpreted in terms of compositional fluctuations in the materials [7,8]. However, recent cross-sectional scanning tunneling microscopy (STM) results [9] have shown little evidence of clustering in GaAsN alloys.

In previous work [9] we used cross-sectional STM to image N atoms in $GaAs_{0.983}N_{0.017}$ alloys. Nitrogen atoms in the first and third planes relative to the $(1\bar{1}0)$ surface were identified. In this work, we further describe the determination of the positions of about a 1000 first and third layer N atoms in a continuous strip of alloy material. We statistically analyze this data in two different ways and we find the arrangement of N atoms is consistent with that expected from a random occupation with the exception that there is a slightly enhanced occurrence of [001]-oriented nearest-neighbor N pairs. Furthermore, we use voltage dependent imaging to probe features we associate

with second-plane N atoms. We propose a simple structural model to explain the appearance of second-plane N atoms in the STM images.

Various groups have shown that performing a post-growth anneal on GaAsN and InGaAsN alloys can dramatically improve the optical quality of the materials [10]. In some cases PL peak intensity can rise by a factor of a thousand [11]. Here, we use STM and scanning tunneling spectroscopy (STS) to probe as-grown and annealed InGaAsN samples. We find the distribution of N atoms is consistent with that seen in GaAsN. Spectroscopy results show significant band gap reduction and we observe a conduction band edge resonance associated with N_{As}. We find little difference in filled state STM images and spectra between annealed and as-grown InGaAsN samples.

2 Experiment

The GaAsN sample was grown on a n-type GaAs(001) substrate by metal organic vapor phase epitaxy (MOVPE) at temperatures ranging from 530 to 570° C using TMGa, TBAs or AsH_3, and tertiarybutylhydrazine (TBHy) under hydrogen carrier gas. Details of material growth and characterization may be found in Ref. [12]. The sample was made up of two 18 nm thick GaAsN quantum wells separated by a 52 nm thick GaAs spacer. One well had a nitrogen concentration of 1.7% and the second well had a nitrogen concentration of 2.8%. The GaAs buffer and cap layers were Si doped to a concentration of 2×10^{18} cm^{-3} while the wells and spacer were undoped. Layer thicknesses and N concentrations were determined by high-resolution x-ray diffraction (HRXRD) and were in fair agreement with STM measurements of the same quantities. STM data was obtained by cleaving the sample *in situ* to expose a $(1\bar{1}0)$ plane. Obtaining atomically flat cleavage faces was relatively difficult, probably due to the mismatch in strain and/or elastic constants between the GaAs and the GaAsN. Large cleavage steps located in or near the alloy layers often occurred, and smaller cleavage related defects within the GaAsN layers were also seen (these cleavage related defects were more numerous in the high N-content layer, and for that reason our study has focussed on the low N-content layer). The STM studies were performed using PtIr probe tips, at a constant current of 0.1 nA.

The InGaAsN samples were grown on GaAs (001) substrates via MOVPE at a temperature of 580° C using TMGa, TMIn, AsH_3, and dimethylhydrazine (DMHy) under hydrogen carrier gas. Additional details of material growth and characterization may be found in Ref. [13]. The samples consisted of a 1 μm thick InGaAsN layer grown on top of a 0.2 μm thick GaAs buffer layer. The substrates were doped with Si to a concentration of 2×10^{18} cm^{-3}. The growth layers were doped with Se from H_2Se to a concentration $\geq 3 \times 10^{18}$ cm^{-3}. Each InGaAsN sample was nominally 4 % In and 1 % N. These concentrations were determined by HRXRD and compared well with STM observations of the samples.

3 Results and Discussion

3.1 Nitrogen Atom Arrangement

Statistical analysis of the arrangement of N atoms in the $GaAs_{0.983}N_{0.017}$ alloy layer has been performed as previously described [9]. We analyze a 400 nm long continuous strip of alloy layer, marking the location of all first- and third-layer N atoms. An example of such data is shown in Fig. 1. Figure 1(a) shows the raw STM image, and Fig. 1(b) shows the image on which a grid of unit cell positions (determined by Fourier analysis of the image) has been superimposed. The nitrogen atoms appear as the small black depression in the image, marked by the small white squares in Fig.

1(b). As discussed elsewhere [9], the depth of the depressions associated with the N atoms fall into two categories, the deeper ones associated with N atoms in the uppermost surface plane (the first plane), and the shallower ones associated with N atoms in the third plane. Also marked in Fig. 1 is a cleavage induced defect. For the analysis presented below, we include the locations of all N atoms as well as the locations of the cleavage-induced defects which result in "dead space" in the images.

The complete map of the analyzed $GaAs_{0.983}N_{0.017}$ layer is shown in Fig. 2. First- and third-plane N atoms are distributed throughout the alloy layer. The goal of our analysis is to ascertain whether or not the N atoms are randomly distributed in the layer. Before proceeding with this analysis, we note that the alloy layer shown in Fig. 2(a) displays some amount of both nonplanarity and thickness variation. The former is evident from the large (multiple unit cell) steps seen at the lower alloy/GaAs interface (right side of Fig. 2(a)), particularly at vertical unit cell positions of 100, 350, 670, and 840. These steps arise from the substrate. The nonplanarity is more or less maintained at the upper alloy/GaAs interface. Some thickness variation of the alloy layer is also evident in the data of Fig. 2(a). This effect might possibly be coupled with the nonplanarity. Data from other regions of the alloy separated by many mm from that shown in Fig. 2 tended to display somewhat less nonplanarity and thickness variation, although a long strip of very high quality images was not obtained from those areas, so that data could not be used for the analysis below.

One means of analyzing the distribution of N atoms is to compute the number of N atoms in a window of fixed size, and then to move that window over the alloy layer. Results for this type of analysis, using a window of size 23×20 unit cells, are shown in Fig. 2(b). We plot the number of nitrogen atoms in the window, N_W, as a function of window position. The window is moved on the slightly tilted path shown by the dashed rectangle in Fig. 2(a). We choose this particular path to minimize the effects of nonplanarity of the alloy layer. A first order correction is made to account for the dead area at each window position, by multiplying N_W by the total window area divided by the difference between total window area and dead area.

From the distribution of N_W values, such as that shown in Fig. 2(b), we can compute the mean, $\langle N_W \rangle$, and standard deviation, σ_{NW}. Results for those quantities are shown in Fig. 3, as a function of the vertical size of the window. For a truly random arrangement of N atoms we would expect $\langle N_W \rangle^{1/2} = \sigma_{NW}$. As seen in Fig. 3 this equality is nearly satisfied by the data. The small deviations from this equality arise, we believe, from residual effects of the nonplanarity and thickness variations in the data. For example, if we assume a narrower window than that shown in Fig. 2(a), and redo the computation, the computed σ_{NW} values for window sizes near 100 are more nearly equal to $\langle N_W \rangle^{1/2}$, since nonplanarity effects are then minimized. We conclude that the arrangement of N atoms appears to be accurately random, at least according to the analysis of Fig. 3.

Another type of statistical analysis which can be performed on the data is to count the number of N-N pairs of a given separation. We have previously discussed this analysis in detail [9], and will not repeat the discussion here. For our prior analysis we showed results in which the first-plane and third-plane N atoms were lumped together. Here, we present results for the analysis in which the two planes are treated separately, as shown in Fig. 4. We show the number of N-N pairs of a given separation, divided by the number of equivalent sites of each separation. The results are consistent with those obtained in the prior analysis: we see a slight enhancement in the number of [001]-oriented nearest neighbor pairs, but aside from this feature the data is consistent with a ran-

dom arrangement of the nitrogen atoms.

3.2 Voltage Dependent Imaging – Detection of Second-Plane Nitrogen

Along with first- and third-plane N atoms we have reported features in the filled state STM images which we associate with second-plane N atoms. Such features appear as small kinks in the anion rows where the As atoms have been shifted a small fraction of a unit cell. To further investigate these features we scanned the surface anion and cation sublattices simultaneously using voltage dependent imaging.

Figure 5 shows two sets of images acquired simultaneously at sample voltages of -2.5 and +1.5 V. In the first set, the negative bias images (a) shows the anion sublattice where several N atoms are visible. The positive bias image (b) shows the cation sublattice. If the two images are compared it can be seen that the empty state image displays relatively little height variation around the N atoms. However, visible in the empty state image are pairs of bright cations. Several of these pairs are marked with arrows. The locations of these pairs do not correspond to those of a first plane or third plane N atoms.

Figure 5(c) and (d) shows a set of simultaneously acquired filled and empty state images with a higher resolution than in Figs. 5(a) and (b). If a single cation pair is examined it can be seen that the atoms in the pair are separated by one atomic row and there appears to be a depression in the lattice adjacent to each pair. The apparent height of the atoms above the plane of the surface is about 0.2 Å. The depression depth is roughly 0.1 Å. If the same location is investigated in the filled state image a feature associated with a second-plane N atom is found. The locations of such features are marked with crosses in both images.

We interpret the voltage-dependent results in terms of second-plane N atoms, as shown in Fig. 6. In the schematic view of the lattice shown there, a nitrogen atom (gray square) has been substituted for a second layer As atom. The N atom is substantially smaller than an As atom, producing a structural rearrangement. A first-plane Ga (atom 1) is shifted toward the N atom, dragging along its neighboring anions and causing the kinked row feature seen in the filled state images. No such kink is seen in the other anions nearby the N atom, but the adjacent first layer cations (atoms 2 and 4) are perturbed. The reason for this is likely associated with the buckling of the Ga-As chains in the $(1\bar{1}0)$ surface. In GaAs$(1\bar{1}0)$ the surface As atoms are raised relative to the surface Ga atoms due to charge transfer from Ga to As [14]. The effect of the second layer N atom may be to slightly unbuckle the nearest Ga-As pairs and subsequently make them appear brighter in the STM image. The effect of the N atom on the middle Ga (atom 3) is difficult to discern in the STM image due to its brighter neighbors. It may be depressed slightly or left unperturbed. Detailed calculation is needed in order to understand the full impact of the N atom on the STM images. We note that the number of bright double-atom features (as in Fig. 5(d)) seen in empty-state STM images is approximately equal to the number of first- or third-plane N atoms observed in the filled state images. The observation supports our identification of the bright empty state features as arising from second-plane nitrogen.

3.3 InGaAsN Imaging and Spectroscopy

In addition to studies of GaAsN, we have also investigated InGaAsN alloy layers. The procedure used to obtain STM images of the InGaAsN samples was similar to that used for the GaAsN sam-

ple. These samples were slightly easier to cleave than the GaAsN sample probably because of the lower N content. However, the surfaces contained many of the same cleavage induced defects seen over the GaAsN sample (i.e. steps, missing or extra atomic rows, and stray atoms).

Figure 7 shows a filled state image of a $In_{0.04}Ga_{0.96}As_{0.99}N_{0.01}$ sample which has been subject to a post-growth anneal at 650 ° C for 10 minutes. The appearance and distribution of N atoms is similar in both the annealed and as-grown InGaAsN samples. Though a detailed analysis comparable to that performed for the GaAsN sample was not undertaken, rough measurements show that the arrangement of N atoms in $In_{0.04}Ga_{0.96}As_{0.99}N_{0.01}$ is similar to that seen in the GaAsN sample. Scattered throughout the image are many raised anions. Two of these raised areas are marked with arrows in the image. These features have been seen in previous cross-sectional STM studies of dilute InGaAs alloys where the elevated anions were thought to be pushed up by subsurface In atoms [15].

Figure 8 contains a set of images acquired simultaneously at –2.5 and +1.2 volts. Consistent with other STM results over InGaAs [15], first-plane In atoms appear as brighter cations in the empty state image. Several are marked with an A. Features seen in voltage dependent imaging over GaAsN are also seen in InGaAsN, namely, the doubled cations which correspond to second plane N atoms (however, no such pair appears in Fig. 8).

To further investigate any difference between annealed and as-grown samples, we preformed scanning tunneling spectroscopy (STS). Figure 9 shows some representative tunneling conductance spectra acquired over both samples. The curve labeled (g) is a typical spectra from the GaAs substrate. The valence and conduction band edges are well defined and are marked by dotted lines. The feature labeled D, near -1.1 volts is due to the well known dopant induced component to the tunnel current [16]. This dopant induced component is sometimes visible in spectra from InGaAsN, for example in curves (b) and (d), however it is often weak or absent. The dopant induced component may be pinched off if it is forced to tunnel through a space charge region caused by surface band bending [17]. Such band bending may be induced by the probe tip, or more commonly in these samples, by proximity to a charged cleavage related defect. The average band gap for both annealed and as-grown samples is found to be 1.2±0.1 eV. The variation in the band gap was probably due to the random nature of the alloy. Some N related features are visible within about 0.5 eV of the conduction band edge. These have been observed previously by STS [18] and are due to a well known N_{As} acceptor level [19]. The appearance of these states was not uniform across the sample. Most likely this is due to small changes in the local alloy concentration in the vicinity of the probe tip (i.e. from nearby N or In atoms). Though there is some variation between individual spectra, there is not much difference between spectra taken over the annealed and spectra taken over the as-grown sample. No evidence of alloy clustering is seen in tunneling spectroscopy.

4 Summary

We investigated N defects in $GaAs_{0.983}N_{0.017}$ and $In_{0.04}Ga_{0.96}As_{0.99}N_{0.01}$ alloys by STM. Statistical analysis of the positions of N defects in $GaAs_{0.983}N_{0.017}$ alloy layers shows that N has a fairly uniform distribution within the layer. STM and STS results from annealed and as-grown $In_{0.04}Ga_{0.96}As_{0.99}N_{0.01}$ samples are consistent with this result. Band gap reduction and an N_{As} conduction band resonance are seen in spectra acquired over $In_{0.04}Ga_{0.96}As_{0.99}N_{0.01}$ alloys. Little difference between annealed and as-grown $In_{0.04}Ga_{0.96}As_{0.99}N_{0.01}$ samples was found in filled state

images or in spectroscopy. A simple structural model involving a second-plane N defect has been proposed to explain features seen in voltage dependent STM images.

5 Acknowledgements

We acknowledge C. Kramer for his contributions to the growth of the InGaAsN material. This work was supported by the National Science Foundation (grant DMR-9985898).

[1] S.-H. Wei and A. Zunger, Phys. Rev. Lett. **76**, 664 (1996).

[2] S. R. Kurtz, A. A. Allerman, E. D. Jones, J. M. Gee, J. J. Banas, B. E. Hammons, Appl. Phys. Lett. **74**, 729 (1999).

[3] Y. Qiu, S. A. Nikishin, H. Temkin, N. N. Faleev, and Yu. A. Kudriavtsev, Appl. Phys. Lett. **70**, 3242 (1997).

[4] I. A. Buyanova, W. M. Chen, B. Monemar, H. P. Xin, and C. W. Tu, Appl. Phys. Lett. **75**, 3781 (1999).

[5] R. A. Mair, J. Y. Lin, H. X. Jiang, E. D. Jones, A. A. Allerman, and S. R. Kurtz, Appl. Phys. Lett. **76**, 188 (2000).

[6] S. R. Kurtz, A. A. Allerman, C. H. Seager, R. M. Sieg, and E. D. Jones, Appl. Phys. Lett. **77**, 400 (2000).

[7] A. M. Mintairov, P.A. Blagnov, V. G. Melehin, and N. N. Faleev, Phys. Rev. B, **56**, 15836 (1997).

[8] S. Francoeur, S. A. Nikishin, C. Jin, Y. Qiu, and H. Temkin, Appl. Phys. Lett. **75**, 1538 (1999).

[9] H. A. McKay, R. M. Feenstra, T. Schmidtling, and U. W. Pohl, Appl. Phys. Lett. **78**, 82 (2001).

[10] X. Yang, J. B. Heroux, M. J. Jurkovic, and W. I. Wang, J. Vac. Sci. Technol. B, **17**, 1144 (1999).

[11] E. V. K. Rao, A. Ougazzaden, Y. Le Bellego, and M. Juhel, Appl. Phys. Lett. **72**, 1409 (1998).

[12] T. Schmidtling M. Klein, U. W. Pohl, and W. Richter, MRS Internet J. Nitride Semicond. Res. **5S1**, W3.43 (2000).

[13] J.F. Geisz, D.J. Friedman, J.M. Olson, S.R. Kurtz, and B.M. Keyes, J. Cryst. Growth, **195**, 401 (1998).

[14] R. M. Feenstra, J. A. Stroscio, J. Tersoff, and A. P. Fein, Phys. Rev. Lett. **58**, 1192 (1987).

[15] K.-J. Chao, C. K. Shih, D. W. Gotthold, and B. G. Streetman, Phys. Rev. Lett. **79**, 4822 (1997).

[16] R. M. Feenstra and J. A. Stroscio, J. Vac. Sci. Technol. B, bf 5, 923 (1987).

[17] R. M. Feenstra, Phys. Rev. B, **50**, 4561 (1994).

[18] R. S. Goldman, B. G. Briner, R. M. Feenstra, M. L. O'Steen, and R. J. Hauenstein, Appl. Phys. Lett. **69**, 3698 (1996).

[19] D. J. Woldford, J. A. Bradley, K. Fry, and J. Thospson, *17th International Conference of the Physics of Semiconductors*, edited by J. D. Chadi and W. A. Harrison (Springer, New Yrok, 1985), p. 627.

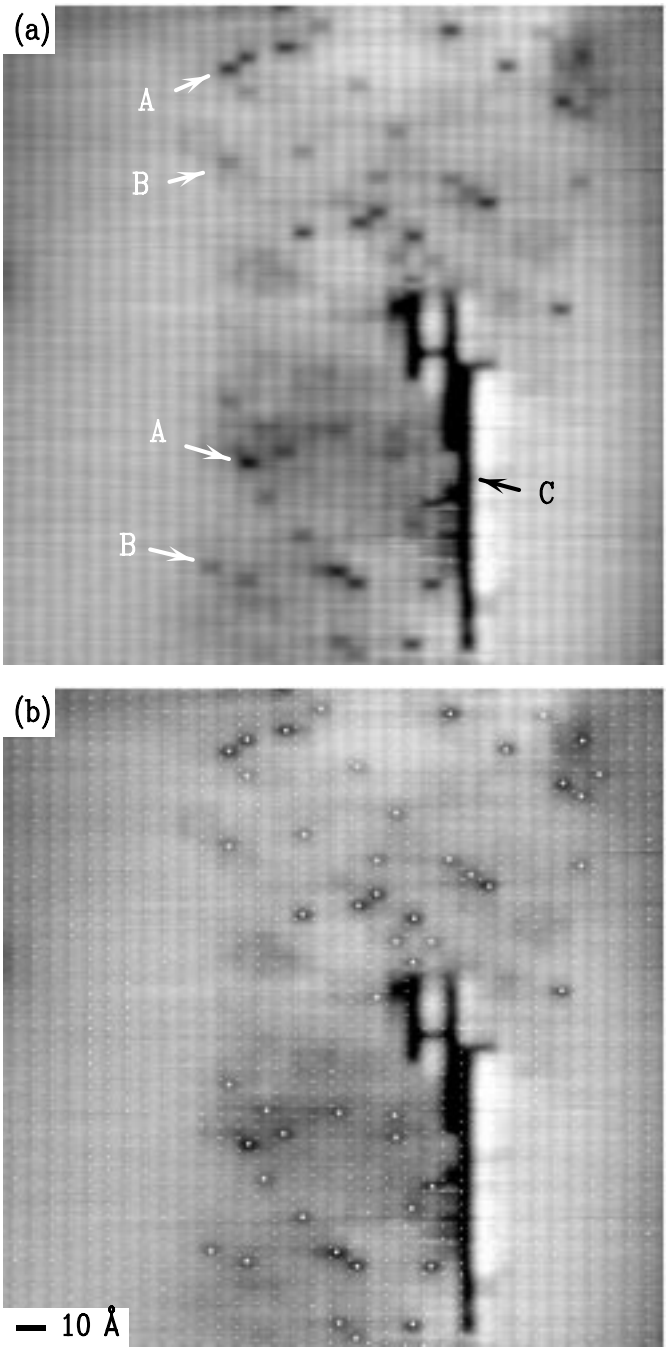

Figure 1 (a) STM image of the $GaAs_{0.983}N_{0.017}$ alloy layer. Growth direction is from right to left. Nitrogen atoms are seen as the small black unit cell size depressions in the image. Several first-plane N atoms are marked A; they are darker than the third-plane N atoms, marked B. A cleavage induced defect is marked by C. The image was acquired at sample bias voltage of –2.3 V and is shown with a gray scale of 1.0 Å. (b) Same STM image as (a), with supeirmposed grid of unit cell positions, and with all N atom locations marked by small white squares.

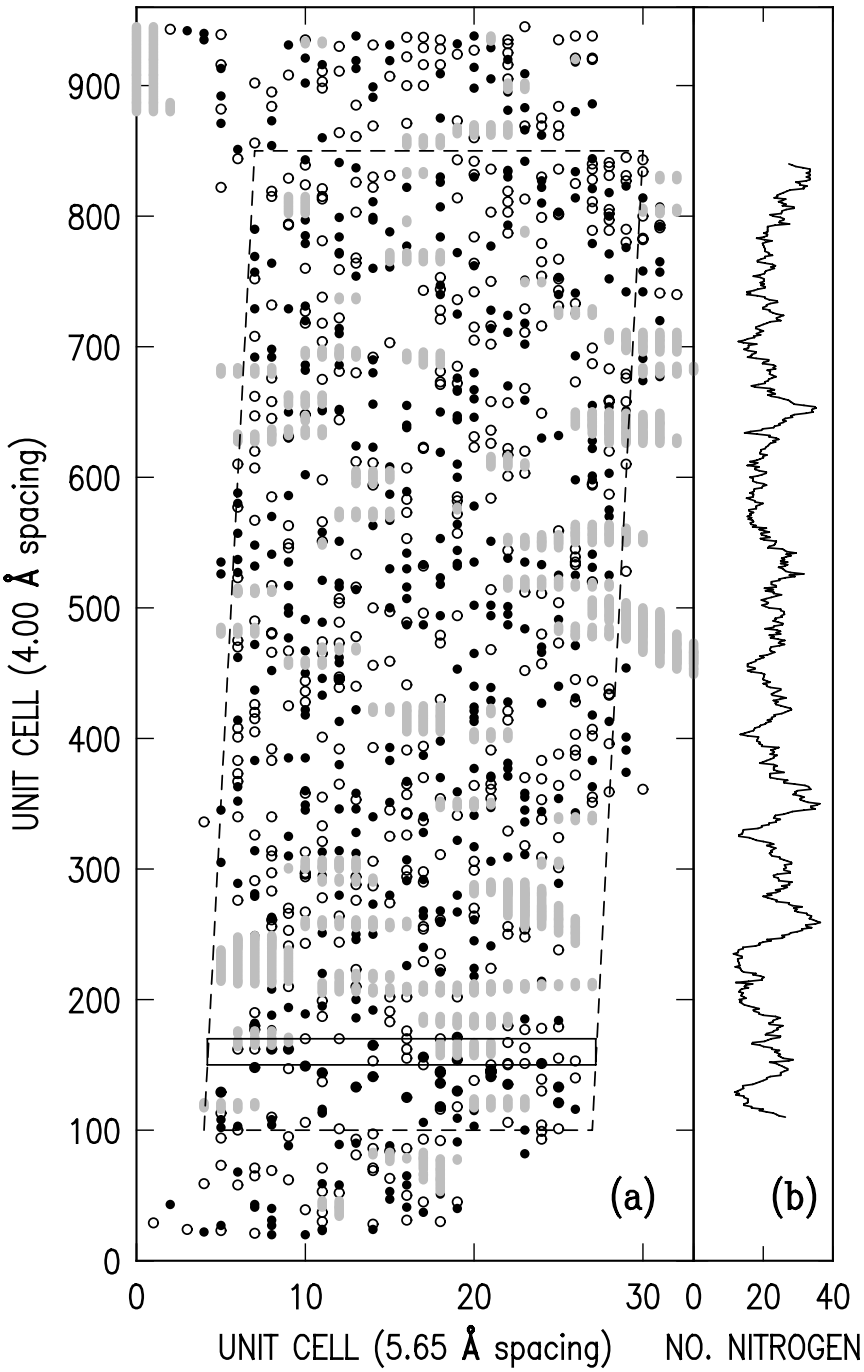

Figure 2 (a) Map of the locations of first-layer N atoms (solid black circles), third-layer N atoms (open circles), and positions of cleavage-induced defects (solid gray circles and lines), for a strip of $GaAs_{0.983}N_{0.017}$ alloy. Note that the vertical axis is compressed by about 10× relative to the horizontal axis. (b) The number of nitrogen atoms in a window of size 23×20 unit cells as shown by the rectangle drawn with solid lines (a), as a function of position along the alloy strip. The position of the window follows the dashed rectangle shown in (a).

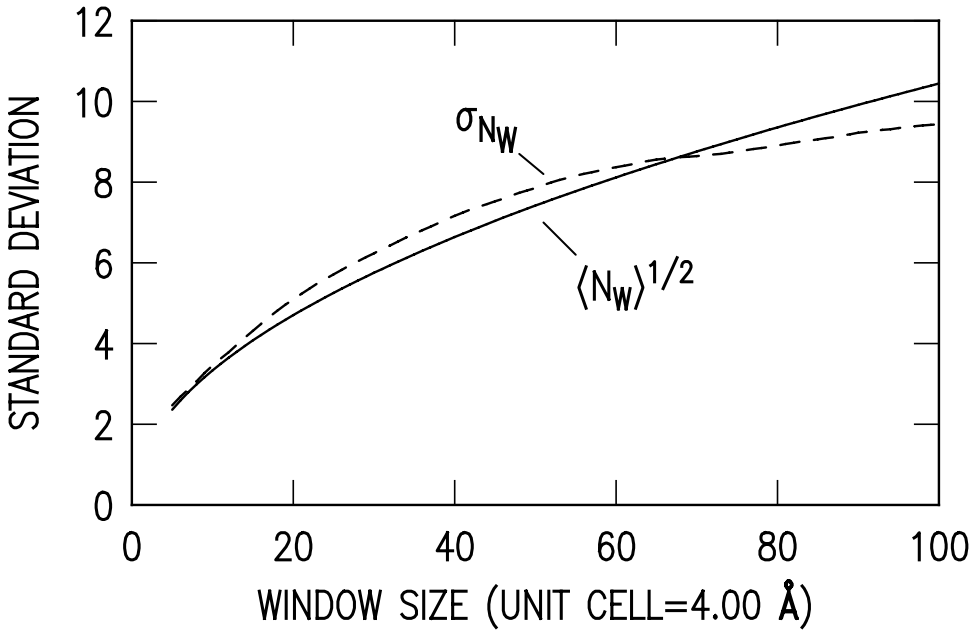

Figure 3 Plot of the square root of the average number of nitrogen atoims in an interval of the $GaAs_{0.983}N_{0.017}$ alloy layer, $<N_W>^{1/2}$, compared to the standard deviation of the number of nitrogen atoms, σ_{NW}. Quantities are plotted versus the interval size (window size).

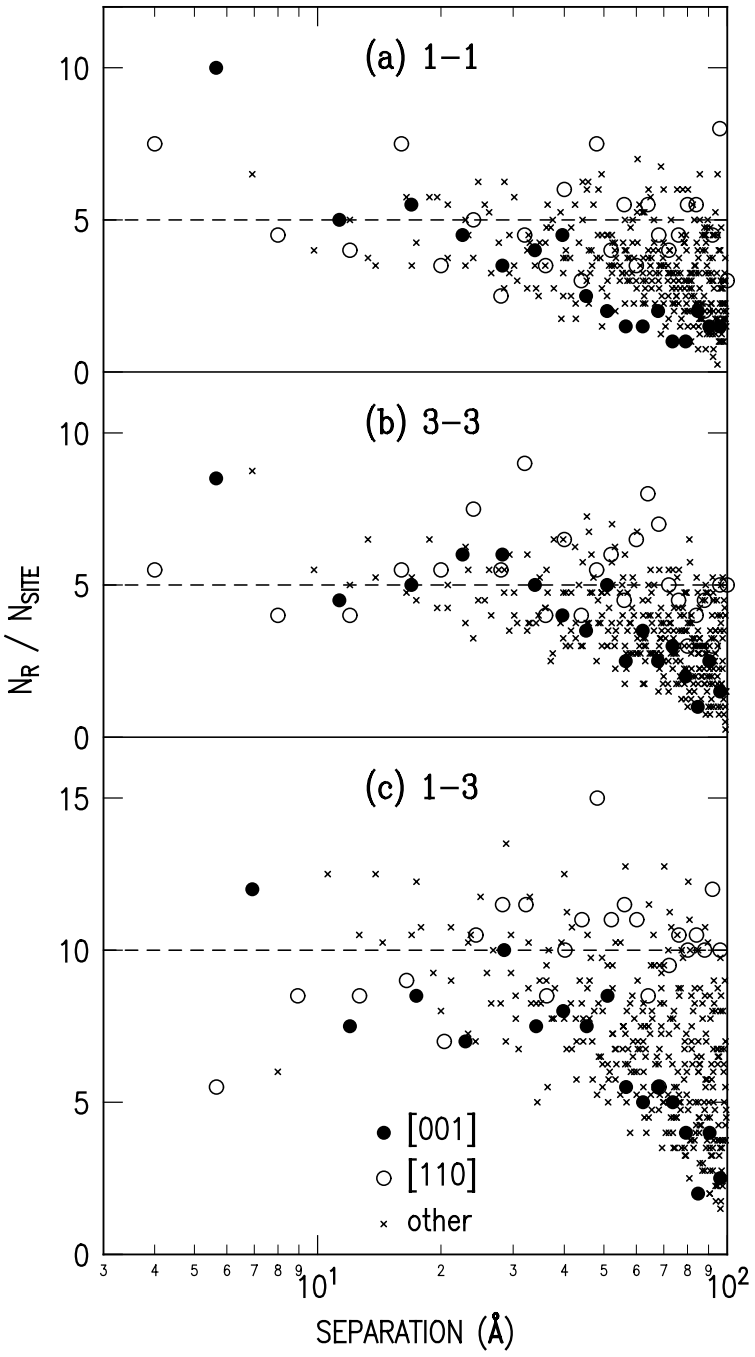

Figure 4 Observed number of N-N pairs N_R of a given separation R, divided by the number of equivalent sites N_{SITE} of each separation. The orientation of the pairs is indicated by the different types of symbols. Uncertainty in the values arises from counting statistics. The dashed lines indicate the expected result for a random arrangement of nitrogen atoms. Results are shown separately for (a) first-plane N atoms, (b) third-plane N atoms, and (c) pairs with one N atom in the first-plane and the other in the third-plane.

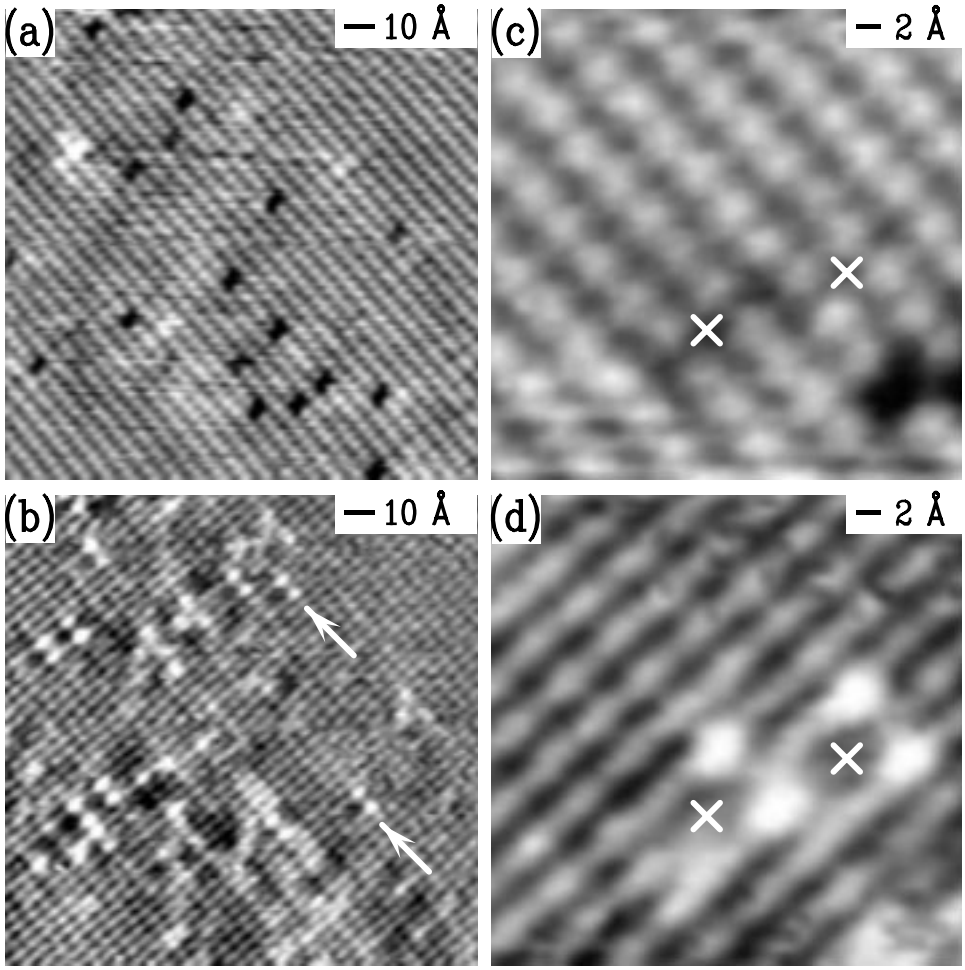

Figure 5 STM images of the $GaAs_{0.983}N_{0.017}$ surface. Both images (a) and (b) were acquired simultaneously at sample voltages of –2.5 and +1.5 V respectively. Similarly for (c) and (d). White arrows mark the locations of features associated with second-plane N atoms in (b). (c) High-resolution filled state image of the $GaAs_{0.983}N_{0.017}$ surface. The corresponding empty state image is shown in (d). White crosses mark the locations of presumed second-plane N atoms. Filled state images (a) and (c) are displayed with a gray scale range of 0.3 Å, and empty state images (b) and (d) are displayed with a gray scale range of 0.4 Å.

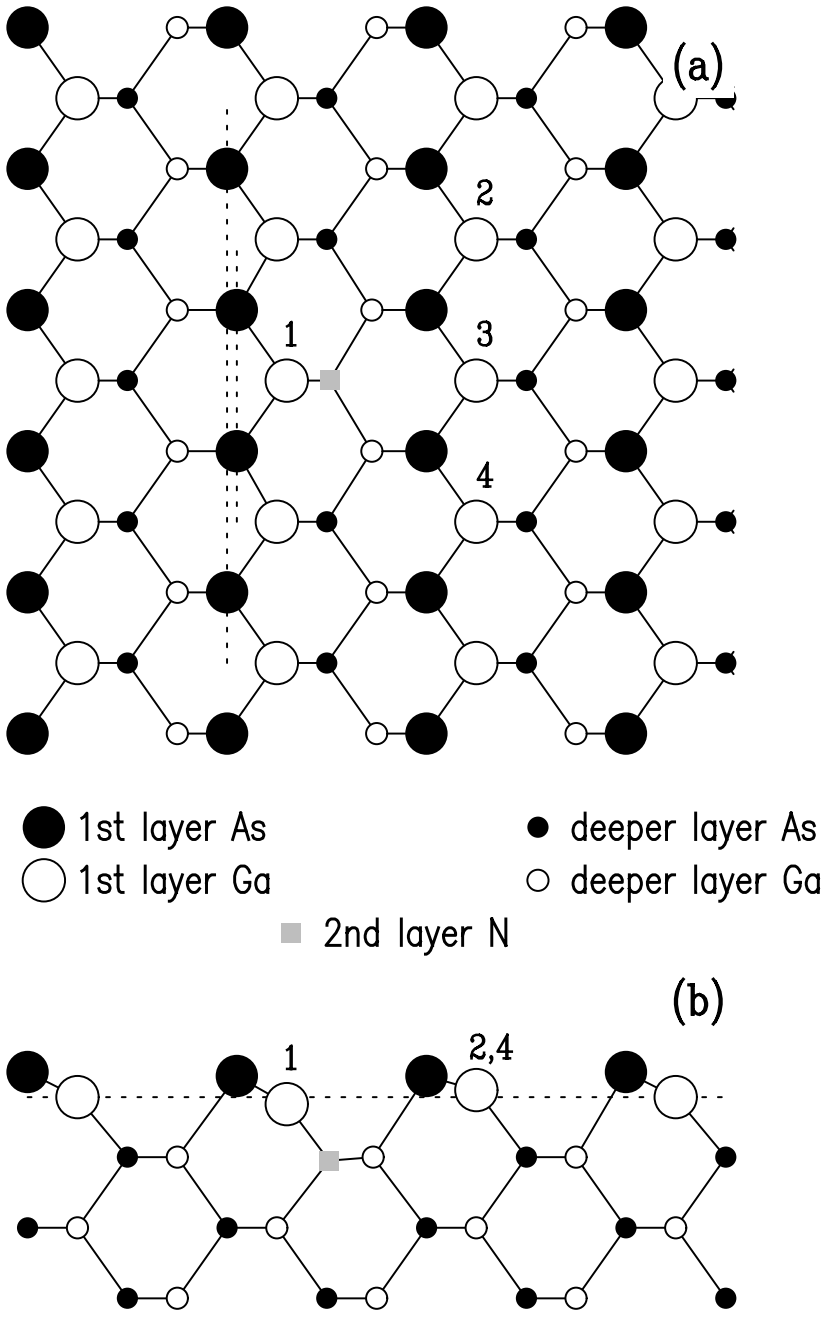

Figure 6 (a) Schematic top view of the GaAsN $(1\bar{1}0)$ surface showing first-plane atoms (large dots) and deeper plane atoms (small dots). A nitrogen atom (gray square) has been substituted for a second-plane As atom. The two nearest As atoms have been shifted toward the N atom a fraction of a unit cell (indicated by the dotted lines) replicating the kink feature seen in filled state STM images. Surface Ga atoms 2 and 4 appear brighter in empty state images while 1 appears darker relative to the surface plane. The appearance of atom 3 is discussed in the text. (b) Side view showing the buckled Ga-As surface pairs and deeper planes in GaAs. A second-plane N atom has changed the buckling in nearby Ga-As pairs.

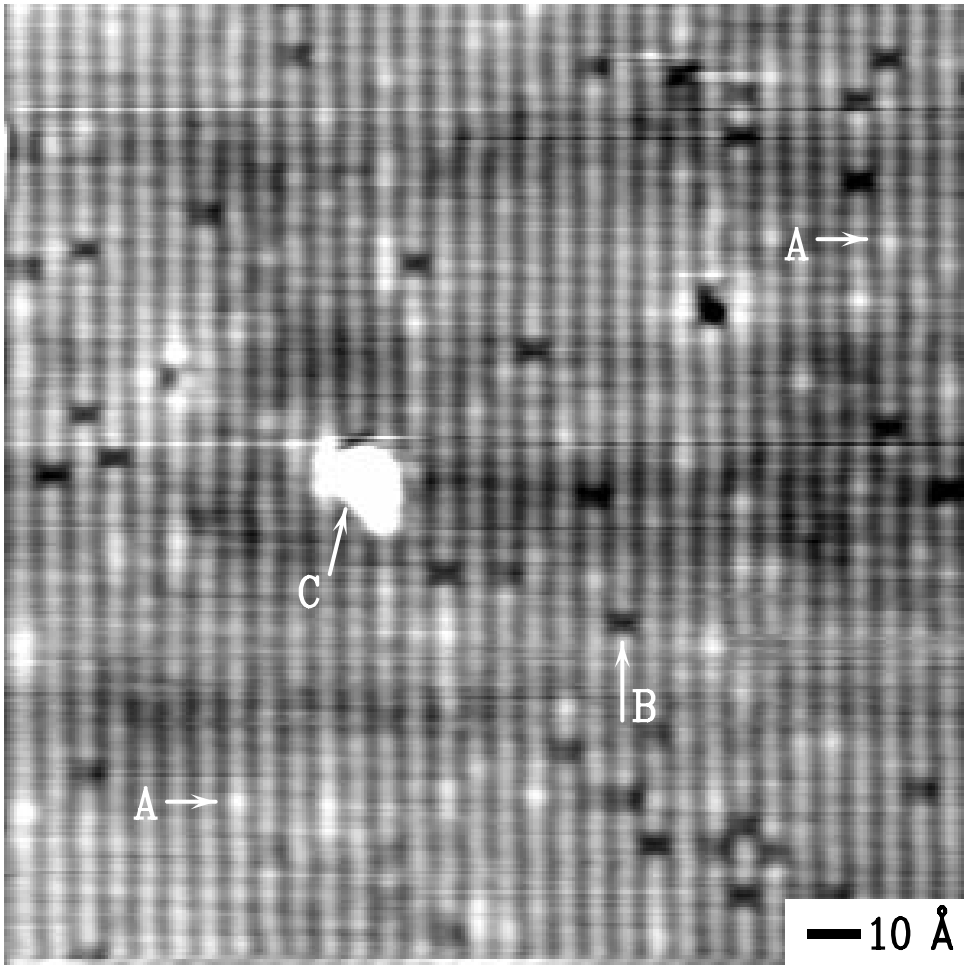

Figure 7 STM image of the $In_{0.04}Ga_{0.96}As_{0.99}N_{0.01}$ surface from an annealed sample. The distribution of N atoms is consistent with that seen in $GaAs_{0.983}N_{0.017}$. The locations of several subsurface In atoms are marked with an A. A single N atom is marked B; a cleavage induced defect is marked C. There was no apparent difference in the disributions of N atoms seen either the annealed or as-grown samples. The image was acquired at a sample bias of –2.5 volts and displayed with a gray scale of 1.0 Å.

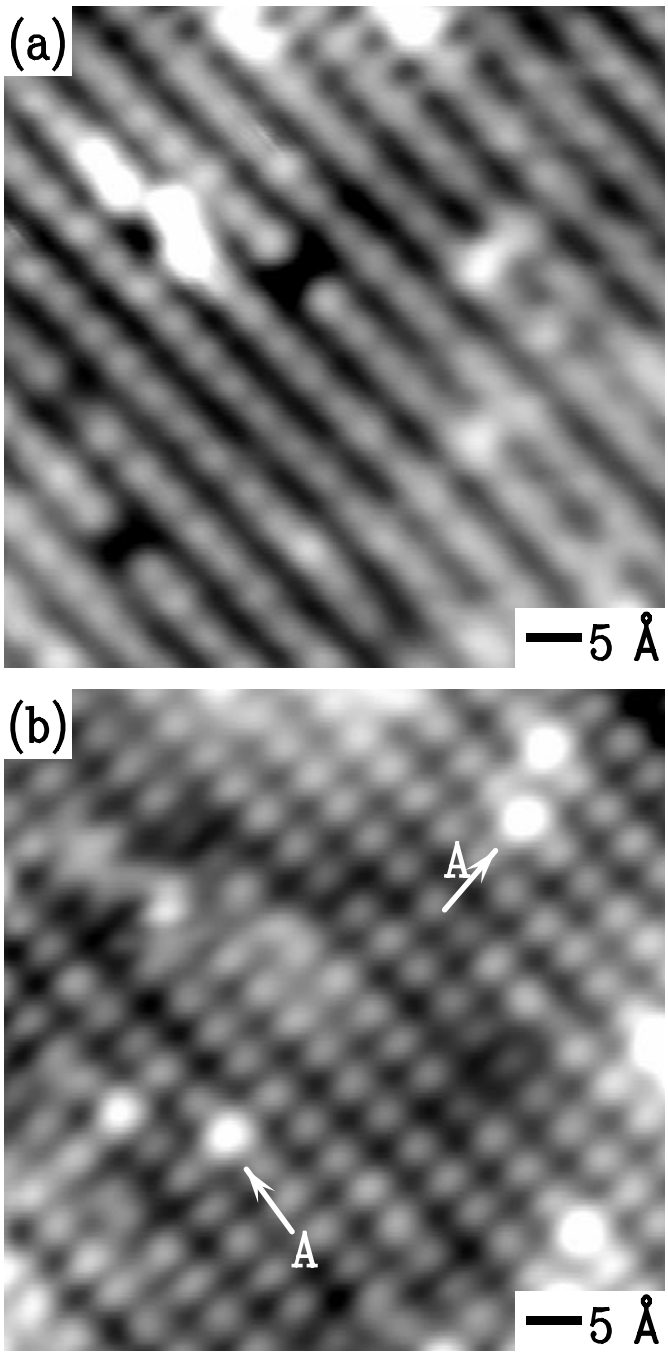

Figure 8 (a) STM images of the $In_{0.04}Ga_{0.96}As_{0.99}N_{0.01}$ surface from an as-grown sample. Both images were acquired simultaneously at samples voltages of (a) –2.5 V and (b) +1.2 V. The locations of several surface In atoms are marked with A in the empty state image. Images are displayed with gray scale ranges of (a) 0.6 Å and (b) 0.7 Å.

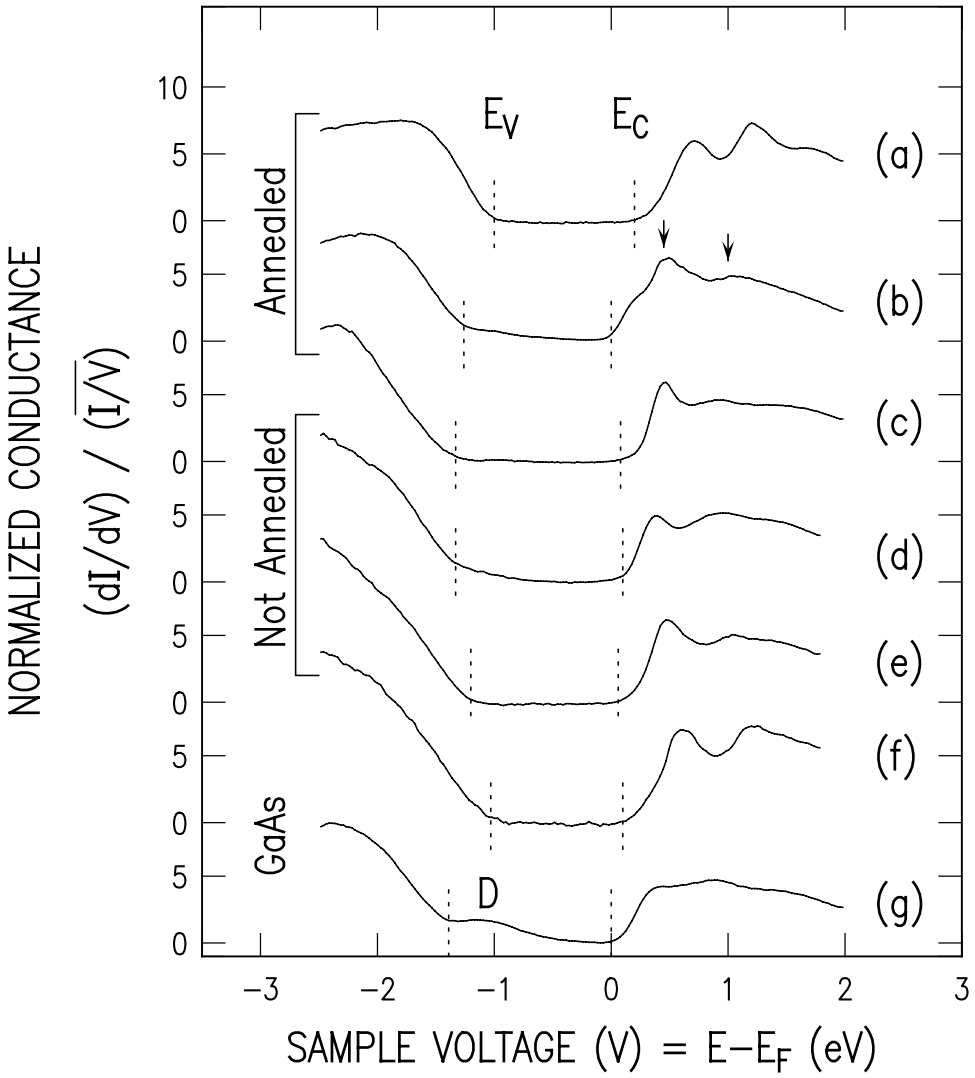

Figure 9 Representative normalized tunneling conductance spectra from annealed and as-grown $In_{0.04}Ga_{0.96}As_{0.99}N_{0.01}$ samples. Curve (g) is a spectra taken over the GaAs substrate. The valence band edge E_v and conduction band edge E_c are marked by dotted lines. The dopant-induced component of the current is labeled *D*.All curves taken over the InGaAsN samples display some band gap reduction compared to GaAs. Arrows indicate features in the InGaAsN spectra near the conduction band edge due to N_{As}. On average there is little difference in spectra taken over the annealed sample compared to spectra taken over the as-grown sample.